

# Effects of diffusion in competitive contact processes on bipartite lattices

M. M. de Oliveira<sup>1</sup> and C. E. Fiore<sup>2</sup>

<sup>1</sup>Departamento de Física e Matemática, CAP, Universidade Federal de São João del Rei, Ouro Branco-MG, 36420-000 Brazil,

<sup>2</sup> Instituto de Física, Universidade de São Paulo, São Paulo-SP, 05314-970, Brazil

## Abstract.

We investigate the influence of particle diffusion in the two-dimension contact process (CP) with a competitive dynamics in bipartite sublattices, proposed in [Phys. Rev. E **84**, 011125 (2011)]. The particle creation depends on its first and second neighbors and the extinction increases according to the local density. In contrast to the standard CP model, mean-field theory and numerical simulations predict three stable phases: inactive (absorbing), active symmetric and active asymmetric, signed by distinct sublattice particle occupations. Our results from MFT and Monte Carlo simulations reveal that low diffusion rates do not destroy sublattice ordering, ensuring the maintenance of the asymmetric phase. On the other hand, for diffusion larger than a threshold value  $D_c$ , the sublattice ordering is suppressed and only the usual active (symmetric)-inactive transition is presented. We also show the critical behavior and universality classes are not affected by the diffusion.

PACS numbers: 05.50.+q, 05.70.Ln, 05.70.Jk, 02.50.Ey

*Keywords:* Contact process, symmetry-breaking, absorbing state, nonequilibrium phase transitions

Submitted to: *J. Stat. Mech.*

## 1. Introduction

Absorbing-state phase transition manifest themselves when a control parameter (such as a creation or annihilation rate) is tuned providing a phase transition from a fluctuating to a state absent of any fluctuation. They have deserved considerable interest in recent years, being related to the description of several phenomena such as population dynamics, epidemic spreading, chemical reactions and others [1, 2, 4, 3], as for the search of experimental verifications [5, 6].

Nowadays it is widely accepted that absorbing transitions in systems with short-range interactions devoid of conserved quantity or symmetry beyond translational invariance belong to the directed universality (DP) class [7]. In another scenario, the so-called DP2 ( $Z_2$ ) universality class embraces systems with two absorbing states linked by particle-hole symmetry, such as branching-annihilating random walks with conserved parity [8], monomer-monomer reaction models [9] and also the voter model [10].

Recently, a bidimensional contact process (CP) which exhibits sublattice symmetry breaking was proposed by de Oliveira and Dickman [11]. In addition to the standard creation and annihilation CP mechanisms, an activation evolving second-neighbors and annihilation depending on the local density are included. Besides the usual absorbing (AB) and active [symmetric] (AS) phases, mean field theory (MFT) and Monte Carlo (MC) analysis predicted the appearance of an unusual active asymmetric (AA) phase in which the distinct sublattices are unequally populated. Remarkably, the symmetric and asymmetric phases are separated by a (critical) transition presenting spontaneous symmetry breaking. Mean field theory (MFT) and simulations revealed the absorbing phase transition belongs to the directed percolation (DP) class, whereas the transitions between active phases fall into the Ising universality class, as expected from symmetry considerations. The model was extended by Pianegonda and Fiore [12], who studied the effects of distinct sublattice interactions on the symmetry breaking phase transition. The changing of interactions can lead to discontinuous phase transitions between the absorbing and active phases, although the criticality is not affected [12].

On the other hand, the effects of particle diffusion in competitive contact processes have not been considered yet. In particular, several works have shown that the diffusion can be a relevant perturbation, affecting drastically the critical behavior [3, 13, 14] or even leading to distinct scenarios for discontinuous phase transitions [16, 15, 17]. With these ideas in mind, in the present work, we consider the influence of local diffusion, aimed at analyzing its effects in another context than previous studies (reentrant phase diagram with active phases sharing distinct features, whose transition is signed by a spontaneous breaking symmetry).

The structure of this paper is organized as follows. In the next section, we review the model and analyze its mean-field theory. In Sec. III we present and discuss our simulation results; Sec. IV is devoted to conclusions.

## 2. Model and Mean-Field Theory

The model is a stochastic interacting particle system defined on a square lattice, with each site either occupied by a particle or vacant. Each particle autocatalytically creates a new particle in one of its first- and second-neighbor empty sites with rates  $\lambda_1$  and  $\lambda_2$ , respectively. In a bipartite sublattice,  $\lambda_1$  is the rate of creation in the opposite sublattice, while  $\lambda_2$  is the rate in the same sublattice as the replicating particle. Note that unequal sublattice occupancies are favored for  $\lambda_2 > \lambda_1$ . An occupied site becomes empty at a rate of unity, independent of the neighboring sites. In addition to the intrinsic annihilation rate of unity, there is a contribution of  $\mu n_1^2$ , where  $n_1$  is the number of occupied first neighbors. In order to understand the meaning of this term in the stabilization of asymmetric phase, let us consider a scenario in which the occupation fraction  $\rho_A$  of sublattice A is much larger than that of sublattice B. Particles created in sublattice B will die out in a short time, stabilizing the unequal sublattice occupancies. From the above, it is clear that appropriate quantities for characterizing the phase transitions are densities of sublattices A and B,  $\rho_A$  and  $\rho_B$ , respectively. The total density of particles is given by  $\rho = \rho_A + \rho_B$ . In a phase absent of particle creation, we have  $\rho_A = \rho_B = 0$ , consistent with the absorbing state. For distinguishing the sublattice occupations, a remarkable quantity is  $\phi = |\rho_A - \rho_B|$ . In the absorbing and the active *symmetric* (AS) phases, it follows that  $\phi = 0$ , implying that there is no difference between the population of sublattices. Otherwise, in an active *asymmetric* (AA) phase,  $\phi \neq 0$  (since both sublattices are unequally occupied). Therefore, we can use  $\phi$  as an order parameter for featuring a *spontaneous breaking symmetry* transition.

The first inspection over the diffusion effect can be achieved by deriving the one site MFT equations. For a lattice of coordination number  $q$  ( $q = 4$  in the square lattice), given by the following coupled equations

$$\frac{d\rho_A}{dt} = -[1 + \mu q^2 \rho_B^2 + D\rho_B^*] \rho_A + [(\lambda_1 + D)\rho_B + \lambda_2 \rho_A] \rho_A^* \quad (1)$$

and

$$\frac{d\rho_B}{dt} = -[1 + \mu q^2 \rho_A^2 + D\rho_A^*] \rho_B + [(\lambda_1 + D)\rho_A + \lambda_2 \rho_B] \rho_B^* \quad (2)$$

where  $\rho_A^* = 1 - \rho_A$  and  $\rho_B^* = 1 - \rho_B$ . Note these equations are symmetric under  $\rho_A \rightleftharpoons \rho_B$ . Using the above definitions of  $\rho$  and  $\phi$ , we obtain

$$\frac{d\rho}{dt} = (\Lambda - 1)\rho - \frac{\Lambda}{2}\rho^2 - \frac{\Delta}{2}\phi^2 - \frac{1}{4}\mu q^2(\rho^2 - \phi^2)\rho, \quad (3)$$

and

$$\frac{d\phi}{dt} = \left[ \Delta - 1 - 2D - \lambda_2 \rho - \frac{1}{4}\mu q^2(\rho^2 - \phi^2) \right] \phi, \quad (4)$$

where  $\Lambda \equiv \lambda_1 + \lambda_2$  and  $\Delta \equiv \lambda_2 - \lambda_1$ . Eq. (3) predicts the extinction-survival transition appearing at  $\Lambda = 1$ , giving rise to the AS phase, which is linearly stable for small  $\Delta$ . In the AS phase, the stationary density is given by

$$\rho = \frac{1}{2\kappa} \left[ \sqrt{(\Lambda)^2/4 + 4\kappa(\Lambda - 1)} - (\Lambda)/2 \right], \quad (5)$$

with  $\kappa \equiv \mu q^2/4$ . From Eq. (4), this solution is stable (while the one with  $\phi \neq 0$  is unstable), when

$$a_\phi \equiv \Delta - 1 - 2D - \lambda_2 \rho + \kappa \rho^2 < 0, \quad (6)$$

and the transition to the AA phase occurs when  $a_\phi = 0$ .

Eqs. (3) and (4) lead to the emergence of AA phase transition for intermediate values of creation parameters and lower diffusion rates. It is stable only for an intermediate range of  $\lambda_2$  and  $\lambda_1$ . By further increasing  $\lambda_2$  (for  $\lambda_1$  fixed), both sublattices become majority occupied, engendering a transition from the AA to the AS phases. Fig. 1 shows the behavior of both control parameters  $\rho$  and  $\phi$  exemplifies the above main features for  $\lambda_1 = 0.1$  and  $\mu = 2$ . We observe that the AA phase is strongly dependent on the diffusion rate, in which its range decreases by raising  $D$ . Another point concerns that for small  $D$ , the global density mildly changes in the AA phase, whereas it exhibits a monotonous increasing behavior for the diffusion rates.

In Fig. 2 we show the phase diagram obtained via the MFT (continuous lines), for fixed  $\lambda_1 = 0.1$ . As expected, low values of  $\lambda_2$  constrains the system trapped in the absorbing phase, regardless the diffusion value. By increasing  $\lambda_2$  the system undergoes a phase transition from the inactive to the active symmetric (AS) phase. Similar results are found for other values of  $\lambda_1$ . Note that the AA phase decreases by raising  $D$  and disappears at  $D_{MFT} = 3.47(1)$ , giving rise only to the AS phase. On the contrary, the absorbing-AS transition line exists for all values of  $D$ . In all cases, MFT predicts continuous phase transitions.

It is important to note that this *one-site* MFT neglects all correlations between nearest-neighbor sites. In the model, the inhibition term depends on the local density, but in the MFT it appears depending only on the global density. Therefore, the contribution of the inhibition term is more significant (which plays an important role in a sublattice ordering) for a larger range of parameters than for the lattice two-dimensional version.

Although MFT provides a correct *qualitative* description of the model, in the following section, we perform numerical simulation to compare phase diagram and critical properties.

### 3. NUMERICAL SIMULATIONS

#### 3.1. Methods

In this work, we performed extensive Monte Carlo simulations of the model on square lattices of linear size  $L = 20, 40, \dots, 320$  sites, with periodic boundary conditions. The simulation algorithm is the following. First, a site is selected at random. If the site is occupied, it creates a particle at one of its first-neighbors with a probability  $p_1 = \lambda_1/W$ , or at one of its second-neighbors with a probability  $p_2 = \lambda_2/W$ , being  $W = (1 + \lambda_1 + \lambda_2 + \mu n_1^2 + D)$  the sum of the rates of all possible events. With a probability  $p_3 = D/W$  one of the first neighbor sites is chosen at random and the

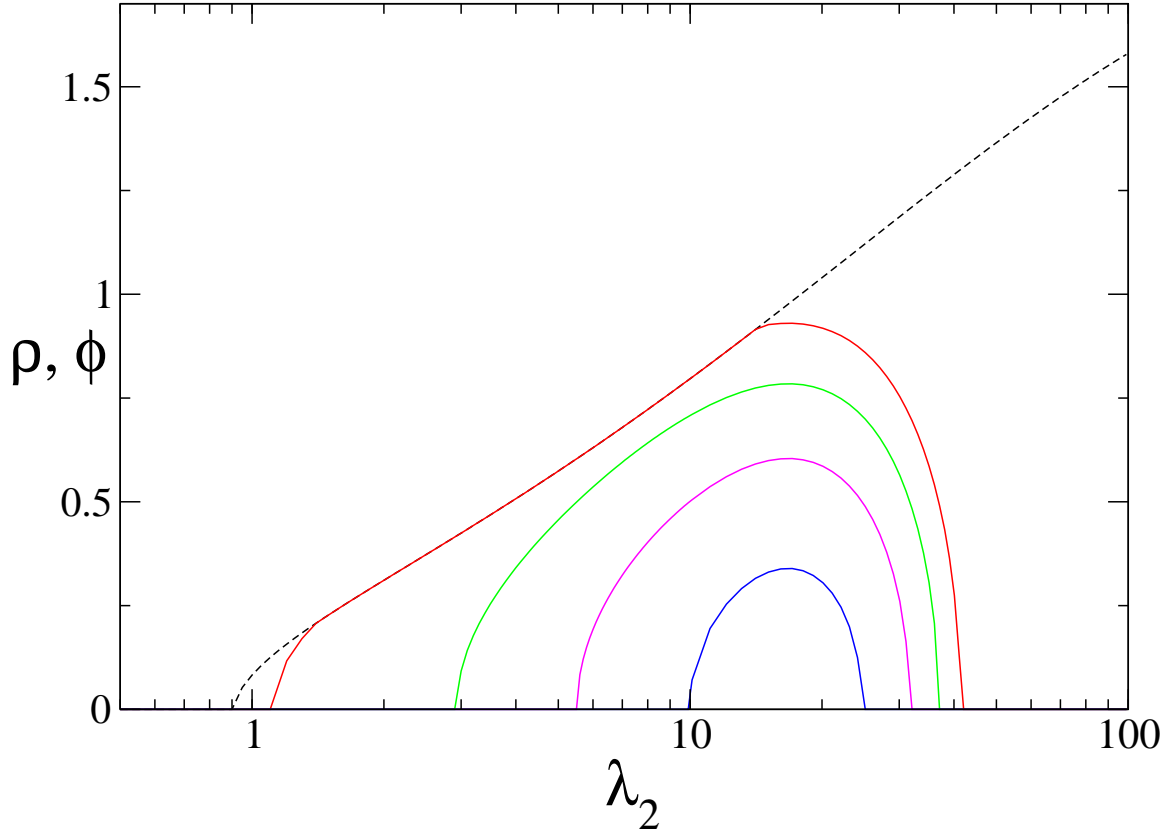


**Figure 1.** (Color online) Stationary densities of  $\rho$  (dashed line) and  $\phi$  (continuous lines) as function of  $\lambda_2$  for  $\mu = 2$  and  $\lambda_1 = 0.1$ . Diffusion rates  $D = 0, 1, 2$ , and  $3$ , from top to bottom.

particle hops to it, provided it is empty. Finally, the above-chosen site is vacated with a complementary probability  $1 - (p_1 + p_2 + p_3)$ , in the case it is occupied  $\ddagger$ . For simulations in the subcritical and in the critical absorbing regimes, we sample the quasi-stationary (QS) regime using the simulation method detailed in [18], to further improve efficiency.

### 3.2. Results and Discussion

As in the MFT, in all cases, numerical results will be obtained for  $\mu = 2$ . Also, the AA phase decreases with the increase of diffusion. Numerical simulations (see Fig. 2) also show the asymmetric-active phase only for intermediate values of  $\lambda_2$ , i.e., the phase diagram is reentrant. Despite the *qualitative* agreement between the phase diagram, MFT overestimates the regions in parameter space corresponding to the active and

$\ddagger$  In order to improve efficiency the sites are chosen from a list which contains the currently  $N_{occ}$  occupied sites; we increment the time by  $\Delta t = 1/N_{occ}$  after each event

ordered phases. In particular the critical diffusion rate (above which the asymmetric-active phase no longer exists) obtained from MFT  $D_{mft}^* = 3.47$  is about an order of magnitude larger than the numerical estimate  $D_n^* = 0.382$ .

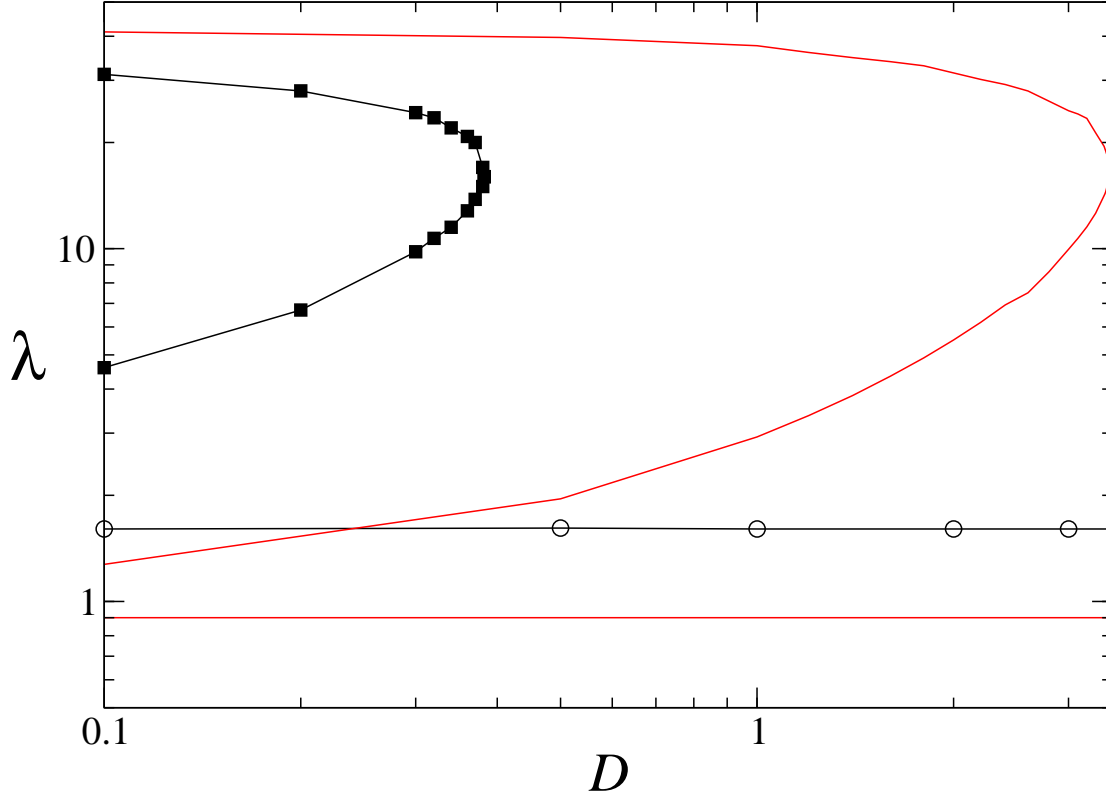


**Figure 2.** (Color online) Phase diagram in the  $D - \lambda_2$  plane for  $\mu = 2$  and  $\lambda_1 = 0.1$ , showing absorbing (ABS), active-symmetric (AS) and active asymmetric (AA) phases. Solid lines (red): results from MFT. Circles: simulation results for the critical points of the absorbing phase transition (black continuous lines are a guide to the eyes). Solid squares: simulation results for the critical points in the AS-AA boundaries (black continuous lines are a guide to the eyes). In the simulations, the critical points are obtained from an extrapolation for  $L \rightarrow \infty$  from system sizes up to  $L = 320$ .

In Figs. 3 and 4 we examine in more details the main features of the phase diagram by inspecting the order parameters  $\rho$  and  $\phi$  as a function of diffusion. For  $D = 0$ , in the active phase,  $\rho$  grows by increasing  $\lambda_2$  until its saturation very close to  $\rho = 0.5$  (at  $\lambda_2 \sim 32.4$ ). This behavior is followed by a maximum of  $\phi$ . Such behavior is a consequence of the inhibition term,  $\mu n_1^2$ , that increases with  $\phi$  and compete with the opposite sublattice term  $\lambda_2$ . By increasing  $\lambda_2$  again, the creation in the opposite sublattice becomes stronger than the inhibition, so that  $\rho$  grows faster and  $\phi$  decreases

towards the vanishing. Adding diffusion, not only  $\phi$  is reduced, but also its maximum. In particular,  $\phi$  vanishes for diffusion  $D > 0.4$ . This change of behavior induced by the  $D$  is closely related to a monotonous increasing of  $\rho$  (unlike the mildly change as verified for  $D = 0$ ). Thus, both MFT and numerical simulations predict the suppression of AA phase for sufficient large diffusion rates.

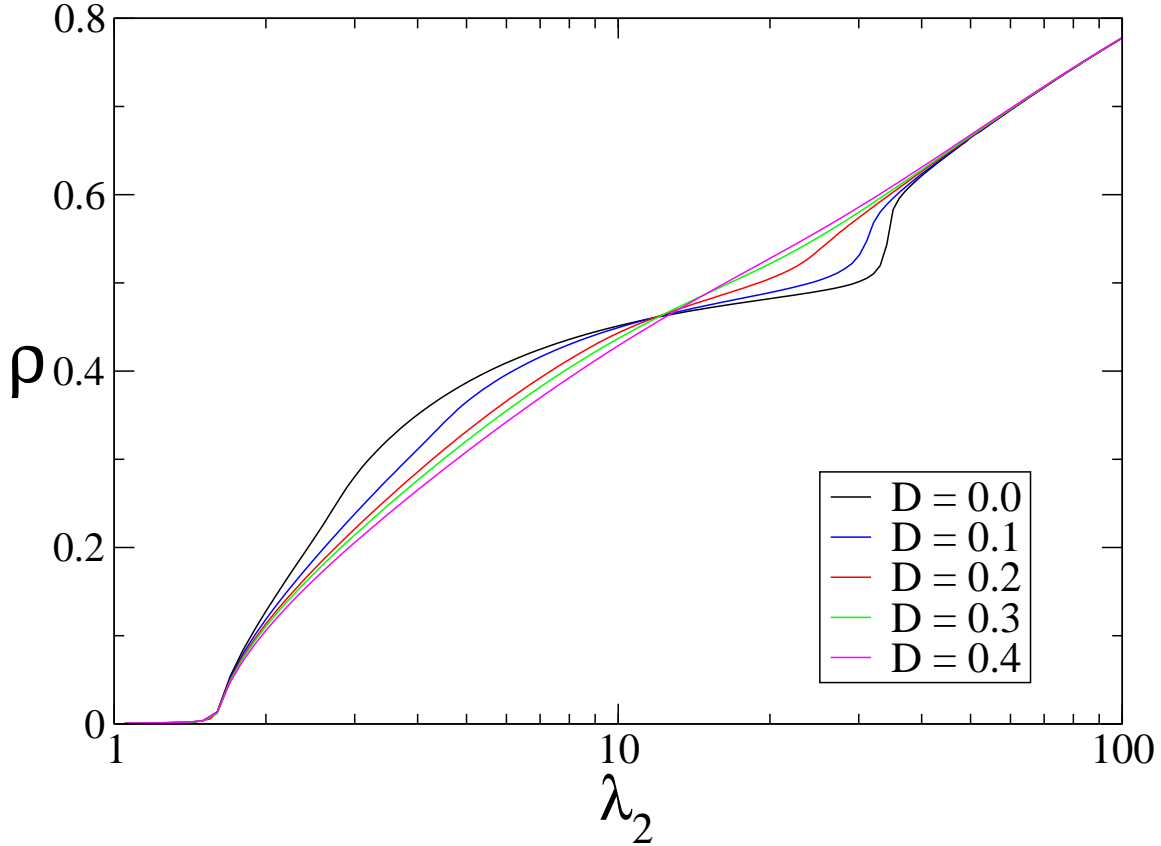


**Figure 3.** (Color online) Density of active sites  $\rho$  for  $\mu = 2$  and  $\lambda_1 = 0.1$ . Linear system size  $L = 160$ .

Now let us examine the critical behavior for the AB-AS, AS-AA and AA-AS phase transitions. Starting with the former case, at the critical point the quasistationary order parameter  $\rho$  decays as a power law  $\rho \sim L^{-\beta/\nu_\perp}$ , being  $\beta/\nu_\perp$  its associated exponent point. In order to locate the transition, we examine the moment ratio  $m = \langle \rho^2 \rangle / \langle \rho \rangle^2$ . At a critical DP like transition,  $m$  assumes a universal value  $m_c = 1.3264(5)$  [20]. Results from Fig. 5(a)-(b) (for  $D = 0.1$  and  $\lambda_1 = 0.1$ ), reveals that curves cross at  $\lambda_{2c} = 1.6250(5)$  for  $m_c = 1.330(5)$ , very close to the above DP value. Also, we obtained  $\beta/\nu_\perp = 0.81(1)$ , in good agreement with the DP value  $\beta/\nu_\perp = 0.797(3)$  [21]. For completeness, we also evaluate the behavior of the lifetime  $\tau$  of the QS state at the

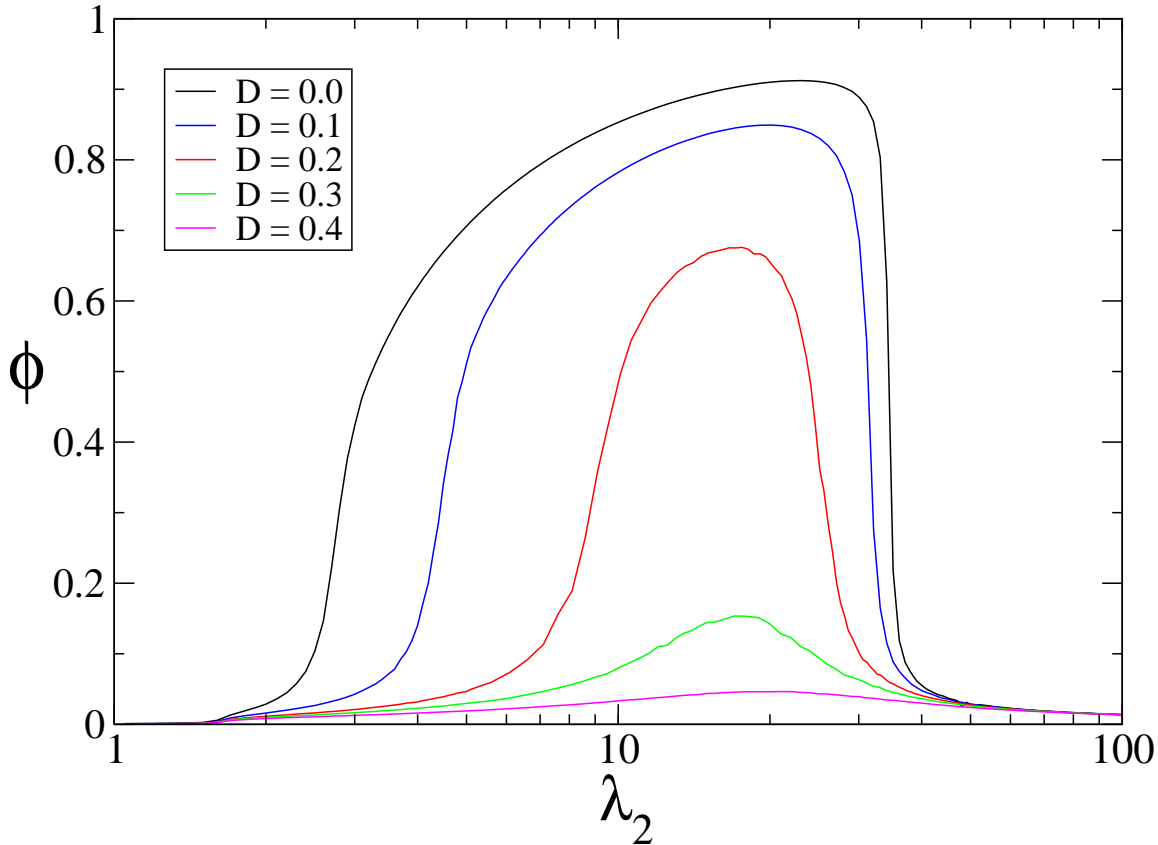


**Figure 4.** (Color online) Density of parameter  $\phi$  for  $\mu = 2$  and  $\lambda_1 = 0.1$ . Linear system size  $L = 160$ .

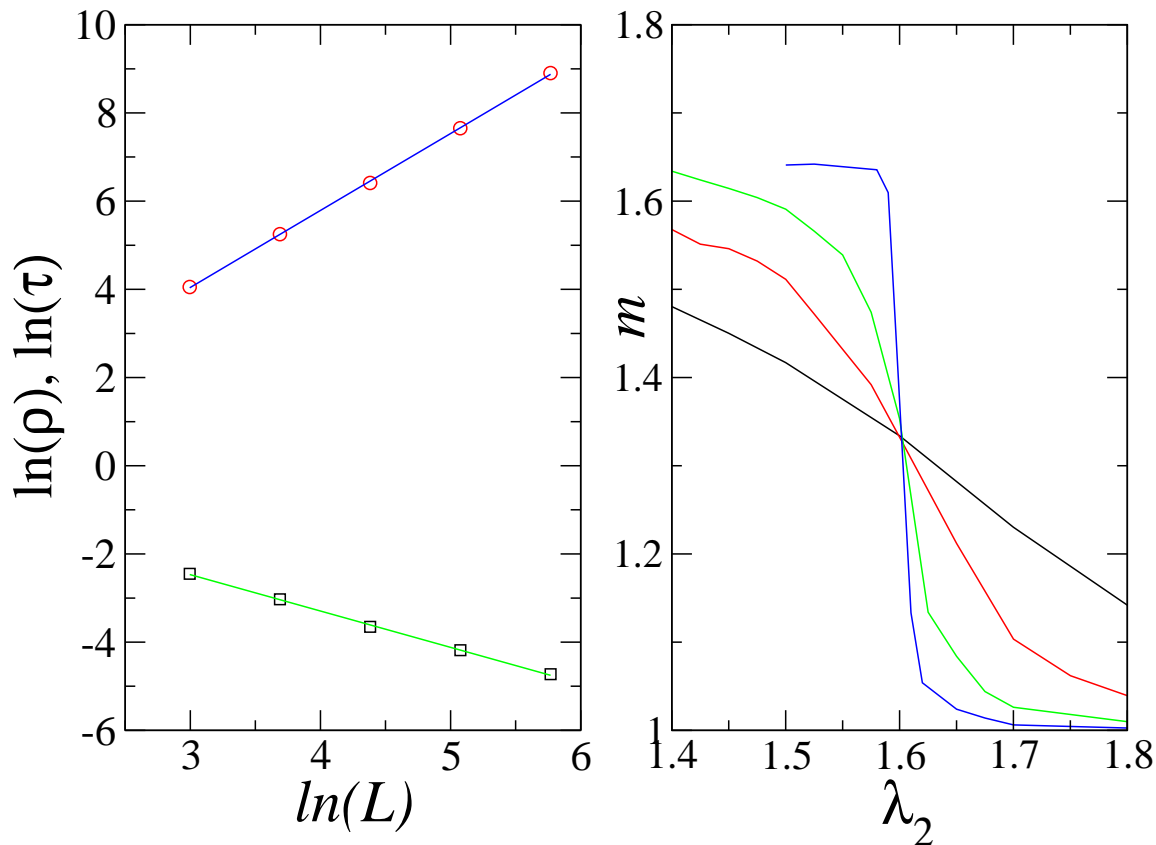
criticality, in which an behavior of type  $\tau \sim L^{\nu_{||}/\nu_{\perp}}$  is expected. From Fig. 5(a), we obtain  $\nu_{||}/\nu_{\perp} = 1.74(2)$  at  $\lambda_{2c}$ , also in very good agreement with the best DP value  $\nu_{||}/\nu_{\perp} = 1.7674(6)$ . Therefore we conclude that the absorbing transition belongs to the DP universality class, as expected.

Fig. 6 exemplify AS-AA and AA-AS phase transitions (also for fixed  $\lambda_1 = 0.1$ ) in which a spontaneous-breaking symmetry is expected. For locating the critical point, we take the reduced Binder cummulant given by [22]

$$U_4 = 1 - \frac{\langle \phi^4 \rangle}{3\langle \phi^2 \rangle^2}. \quad (7)$$

The intersection points of  $U_4$  for successive pairs of sizes depend rather weakly on the sizes, providing a reliable estimate for the critical point and approaching to an universal value as  $L \rightarrow \infty$ . For  $\lambda_1 = 0.1$  and  $D = 0.1$ , the curves for different sizes intersect at  $\lambda_2 = 4.650(5)$ , and again at  $\lambda_2 = 31.27(6)$  when  $L \rightarrow \infty$ , respectively. For the former transition, we found the value  $U_{4,c} = 0.615(10)$ , very close to the universal value





**Figure 5.** (Color online) (a) Scaled critical QS density of active sites  $\ln \rho$  (bottom) and scaled lifetime of the QS state  $\ln \tau$  (top), *versus*  $\ln L$ . Parameters:  $D = 0.1$ ,  $\lambda_1 = 0.1$  and  $\lambda_{2c} = 1.6250$  (b) Moment ratio  $m$  *versus*  $\lambda_2$ . Other parameters same as in (a).

$U_{4,c} = 0.61069\dots$  [23] for the two-dimensional Ising model with fully periodic boundary conditions. On the other hand, the latter transition is signed by a significant smaller value of  $U_{4,c} = 0.55(1)$ , but close to the value reported by Vasquez and Lopez for the general voter model (GVM) [24]. For values of  $\lambda_2$  between the transitions points, the cummulant approaches  $2/3$ , and vanishes outside the asymmetric phase, as expected in an ordered phase that breaks a up-down ( $\mathcal{Z}_2$ ) symmetry.

For obtaining the critical exponents, we measure  $\phi$  and its variance  $\chi = L^d(\langle \phi^2 \rangle - \langle \phi \rangle^2)$  for both AS-AA and AA-AS phase transitions. In all cases, power laws behaviors of type  $\phi \sim L^{-\beta/\nu}$  and  $\chi \sim L^{-\gamma/\nu}$  are also expected at the critical point, being  $\beta/\nu$  and  $\gamma/\nu$  the associated critical exponents, respectively. As shown in Fig. 7, for the former transition we obtained  $\beta/\nu = 0.128(5)$  and  $\gamma/\nu = 1.78(4)$ , in good agreement with the exact value  $\beta/\nu = 1/8$  and  $7/4$  for the Ising universality class in  $d = 2$  [22].

Analysis of AA-AS transition are shown in Fig. 8. In this case, we obtain

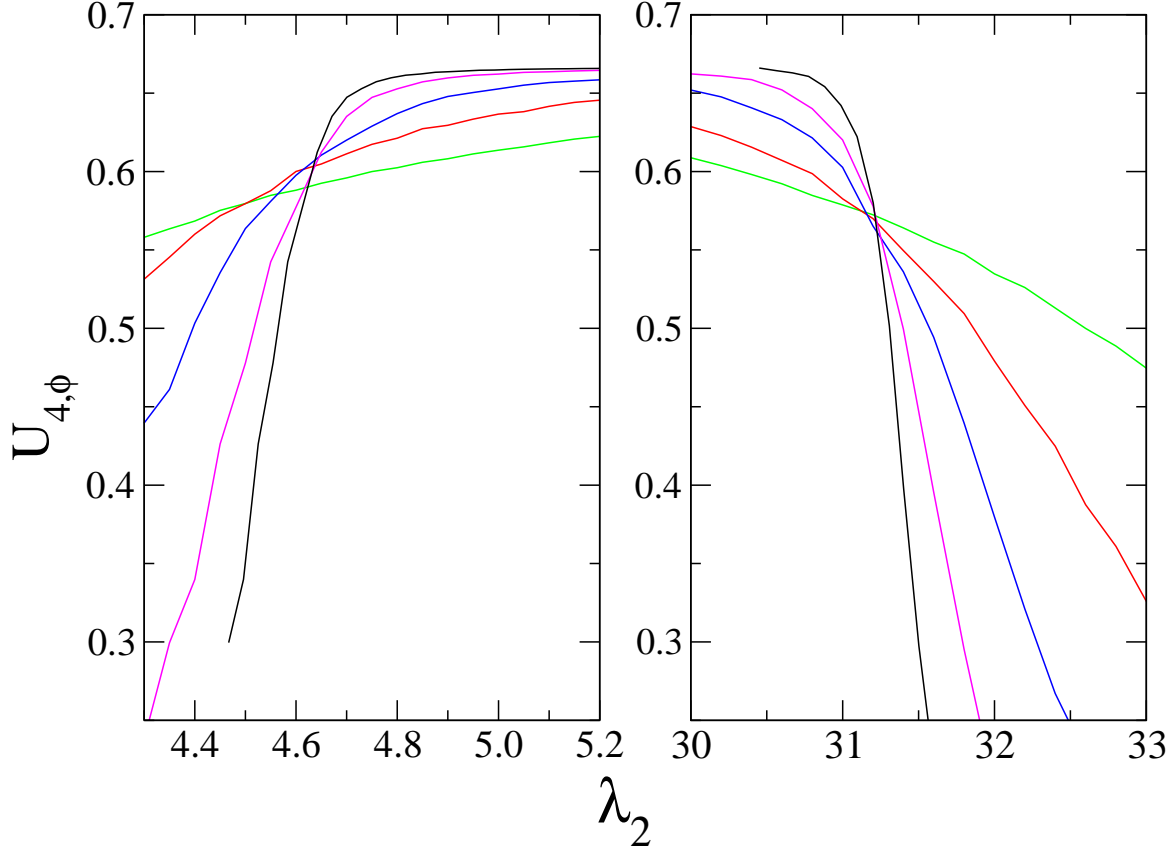


**Figure 6.** (Color online) Binder cumulant  $U_4$  versus  $\lambda_2$  for  $\lambda_1 = 0.1$  and  $D = 0.1$  for the AS-AA (left) and AA-AS (right) phase transitions, respectively. System sizes:  $L = 20, 40, 80, 160$  and  $320$ .

$\beta/\nu = 0.21(2)$  and  $\gamma/\nu = 1.62(4)$  at  $\lambda_{2c} = 31.27(5)$ . These exponents differ from those obtained for the AS-AA transition, but still obey the scaling relation  $\gamma/\nu = d - 2\beta/\nu$ .

#### 4. Conclusions

In this work, we studied, under mean-field theory and extensive simulations, the influence of species diffusion in the phase diagram and critical properties of a contact process living in bipartite sublattices. We observe that low diffusion does not forbid the broken-symmetry phase with sublattice ordering; however it induces a decreasing of asymmetric phase. Further increasing the diffusion  $D$ , there is a threshold value,  $D^*$ , above which no sublattice order occurs. The phase transitions between symmetric-active and absorbing phases belong to the universality class of directed percolation, whereas the first symmetry-breaking transition is found to be Ising-like and the second one seems to belong to the general voter model universality class (this latter transition becomes

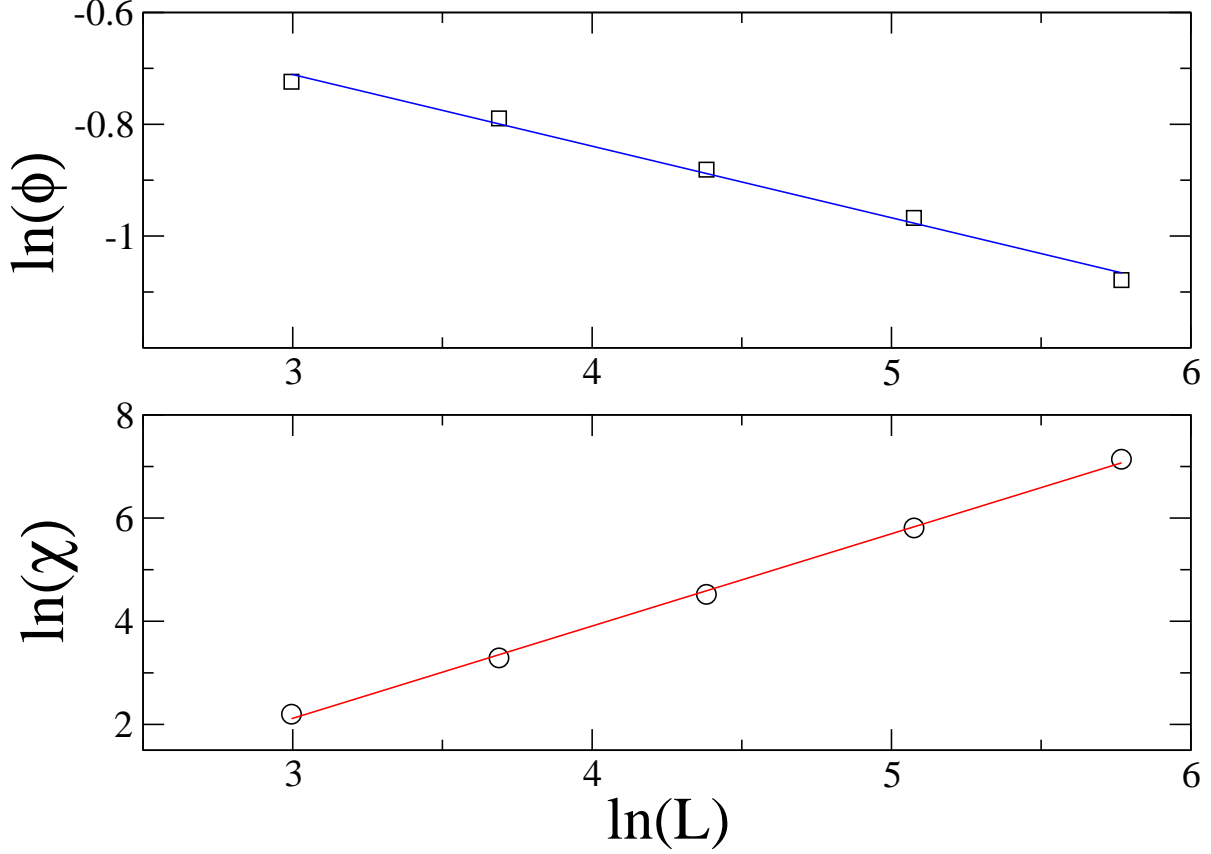


**Figure 7.** (Color online) Finite size scaling for the critical order parameter  $\phi$  (top) and maxima of  $\chi$  (bottom). Parameters:  $D = 0.1$ ,  $\lambda_1 = 0.1$  and  $\lambda_{2c} = 4.65$ .

discontinuous when  $D \rightarrow 0$ ). Thus, despite leading to remarkable changes in the phase diagram, the critical behaviors are preserved for the influence of diffusion.

Interesting extensions of the present work include the study of the model in disordered environments. Disorder can also induce the appearance of spatial [25, 26] and temporal Griffiths phases [27], in which the disordered system exhibit a different behavior than its pure counterpart [28, 29]. We believe that an important question to be investigated is if such kinds of disorder favor the symmetry-breaking and if it changes the nature of the transitions.

## Acknowledgments

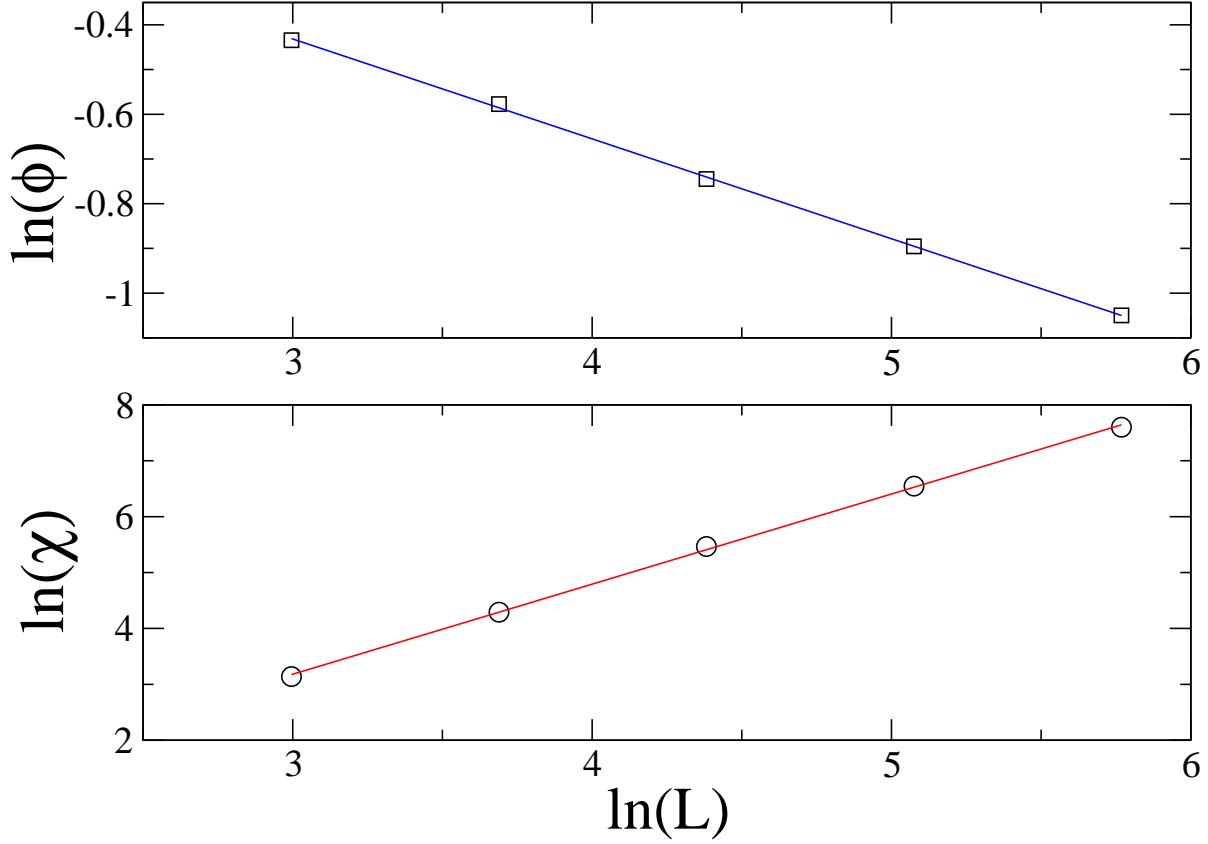


**Figure 8.** (Color online) Finite size scaling for the critical order parameter  $\phi$  (top) and maxima of  $\chi$  (bottom). Parameters:  $D = 0.1$ ,  $\lambda_1 = 0.1$  and  $\lambda_{2c} = 31.27$ .

This work was supported by CNPq, FAPEMIG and FAPESP Brazil. We acknowledge the anonymous referees for their valuable suggestions.

- [1] J. Marro and R. Dickman, *Nonequilibrium Phase Transitions in Lattice Models* (Cambridge University Press, Cambridge, 1999).
- [2] H. Hinrichsen, *Adv. Phys.* **49**, 815 (2000).
- [3] M. Henkel, H. Hinrichsen and S. Lubeck, *Non-Equilibrium Phase Transitions Volume I: Absorbing Phase Transitions* (Springer-Verlag, The Netherlands, 2008).
- [4] G. Ódor, *Rev. Mod. Phys.* **76**, 663 (2004).
- [5] K. A. Takeuchi, M. Kuroda, H. Chaté, and M. Sano, *Phys. Rev. Lett.* **99**, 234503 (2007).
- [6] L. Corté, P. M. Chaikin, J. P. Gollub, and D. J. Pine, *Nature Physics* **4**, 420 (2008).
- [7] H. K. Janssen, *Z. Phys. B* **42**, 151 (1981);  
P. Grassberger, *Z. Phys. B* **47**, 365 (1982).
- [8] H. Takayasu and A. Yu. Tretyakov, *Phys. Rev. Lett.* **68**, 3060 (1992).
- [9] K. E. Bassler and D. A. Browne, *Phys. Rev. Lett.* **77**, 4094 (1996).
- [10] I. Dornic, H. Chaté, J. Chave and H. Hinrichsen, *Phys. Rev. Lett.* **87**, 045701 (2001).
- [11] M. M. de Oliveira and R. Dickman, *Phys. Rev. E* **84**, 011125 (2011).

- [12] S. Pianegonda and C. E. Fiore, J. Stat. Mech. **2014**, P05008 (2014).
- [13] M. Henkel and H. Hinrichsen H, J. Phys. A: Math. Gen. **37**, R117 (2004).
- [14] M. M. de Oliveira and R. Dickman, Phys. Rev. E **74**, 011124 (2006);
- [15] C. E. Fiore and G. T. Landi, Phys. Rev. E **90**, 032123 (2014).
- [16] S. Pianegonda and C. E. Fiore, J. Stat. Mech. **2015**, p08018 (2015).
- [17] M. M. de Oliveira, R. V. dos Santos, and R. Dickman, Phys. Rev. E **86**, 011121 (2012); M. M. de Oliveira and R. Dickman Phys. Rev. E **90**, 032120 (2014).
- [18] M. M. de Oliveira and R. Dickman, Phys. Rev. E **71**, 016129 (2005); Braz. J. Phys. **36**, 685 (2006).
- [19] A. G. Moreira and R. Dickman, Phys. Rev. E **54**, R3090 (1996).
- [20] R. Dickman and J. Kamphorst Leal da Silva, Phys. Rev. E, **58** 4266 (1998).
- [21] R. Dickman, Phys. Rev. E **60**, R2441 (1999).
- [22] K. Binder, Phys. Rev. Lett. **47**, 693 (1981).
- [23] G. Kamieniarz and H.W.J. Blöte, J. Phys. A: Math. Gen. **26**, 201 (1993).
- [24] F. Vazquez and C. Lopez, Phys. Rev. E **78**, 061127 (2008).
- [25] A.G. Moreira and R. Dickman, Phys. Rev. E **54** R3090 (1996);  
R. Dickman and A. G. Moreira, Phys. Rev. E **57** 1263 (1998).
- [26] M. M. de Oliveira and S. C. Ferreira J. Stat. Mech. **2008**, P11001 (2008);  
T. Vojta, A. Farquhar and M. Mast, Phys. Rev. E **79**, 011111 (2009).
- [27] F. Vazquez, J. A. Bonachela, C. López and M. A. Muñoz, Phys. Rev. Lett. **106**, 235702 (2011);  
R. Martínez-García, F. Vazquez, C. López, and M. A. Muñoz, Phys. Rev. E **85**, 051125 (2012).
- [28] J. A. Hoyos and T. Vojta, Europhysics Lett. **112**, 30002 (2015); H. Barghathi, T. Vojta and J. A. Hoyos, Phys. Rev. E **94**, 022111 (2016).
- [29] M. M. de Oliveira and C. E. Fiore, Phys. Rev. E **94**, 052138 (2016).